

## Structural, Thermal and Optical Properties of Pure and Mn<sup>2+</sup> Doped Poly(Vinyl Chloride) Films

*Bhagyasree Kayyapuru<sup>a</sup>, Madhava Kumar Y.<sup>a</sup>, Hussain Basha Mohommad<sup>a</sup>, Gopal Neeruganti O.<sup>a</sup>,  
Ramu Chekuri<sup>a\*</sup>*

*<sup>a</sup>Department of Physics, Vikrama Simhapuri University PG Centre, Kavali 524201, India*

Received: March 22, 2016; Revised: July 20, 2016; Accepted: August 11, 2016

Pure and Mn<sup>2+</sup> doped poly(vinyl chloride) (PVC) polymer films were prepared using the solution cast technique. The prepared samples have been characterized by X-ray diffraction (XRD), UV-Vis Spectroscopy (UV-Vis), Fourier transform infrared (FTIR) Spectroscopy, Thermogravimetric analysis (TGA), Differential Scanning Calorimetry (DSC), Electron Paramagnetic Resonance (EPR) and Scanning Electron Microscopy (SEM) studies. TGA/DSC analysis reveals that the sample is thermally stable upto 350 0C. The morphology of the polymer films was studied by SEM. The optical absorbance of the polymer films was measured in the 200-900 nm wavelength range. The absorption edge, direct band gap and indirect band gap have been evaluated. The FTIR spectrum exhibits several bands characteristics of stretching and bending vibrations of C - Cl, C - H, C = C and O - H groups. The EPR Spectra at room temperature were used to calculate the number of spins and paramagnetic susceptibility as a function of dopant concentration. All the Mn<sup>2+</sup> doped PVC samples exhibit a signal centred at  $g_{\text{eff}} = 1.9$ . The observed variation in the EPR signal intensity is due to the variation in the dopant concentration. The complexation of Mn<sup>2+</sup> ion with the polymer was confirmed by XRD studies.

**Keywords:** *Poly(vinyl chloride), Differential scanning calorimetry, Thermogravimetric analysis*

### 1. Introduction

Recent developments in solid state ionic conductors such as insertion compounds, polymer electrolytes, superionic conductors, and the development of new solid state materials for electrodes have drawn keen interest from the researchers working in the area of electrical power generation and storage systems. Among these, the most recent ones are the polymer electrolytes, also known as poly electrolytes<sup>1</sup>. Polymer electrolytes are promising materials because of their wide applications in electro chromic windows, modified electrodes, sensors, super capacitors, electric vehicles, high vacuum electrochemistry, thermoelectric generators and fuel cells<sup>2,3</sup>.

Poly(vinyl chloride) (PVC) is one of the most important commercial polymers that have wide range of applications. PVC is a linear, thermoplastic and substantially amorphous polymer, with a huge commercial interest due to the accessibility to basic raw materials and its properties. It is used as thermoplastic due to its many valuable properties like low price, good process ability, chemical resistance, good mechanical strength, thermal stability and low flammability<sup>4</sup>. Currently, PVC is one of the world's leading synthetic polymers with global consumption of above 40 million tonnes per annum<sup>5</sup>.

Chlorine – Containing polymers such as PVC are widely used in many fields, namely, water pipes, cable

insulation, floor and roof tiles, packing films and sheets due to their advantages such as non-flammable nature, good performance and low price<sup>6</sup>. However, under the influence of elevated temperature and UV radiation, PVC undergoes an autocatalytic dehydrochlorination reaction, which results in severe discoloration and loss of some properties<sup>7</sup>. Stabilizers can inhibit the degradation or removal of HCl due to their capacity for HCl-adsorption. Although the main used thermal stabilizers are lead salts, metal soaps, organo-tin compounds and rare earth compounds<sup>8,9</sup>. These stabilizers have some drawbacks like toxicity, environmental pollution and high cost. Hence, it is necessary to explore an environmental friendly stabilizer with non-toxicity, economical interest and high efficiency.

Recently, particular attention has been devoted to introduce some structural modification in polymer electrolytes in order to increase their electrical conductivity and improve their thermal, mechanical and electrochemical properties to provide commercial acceptability in electrochemical devices<sup>10</sup>. Several researchers have reported doped polymer electrolytes with enhanced ionic conductivity in PVC based polymer electrolytes<sup>11-18</sup>. As a result, a variety of Polymer electrolytes such as Polymer-salt complexes, gel polymer electrolytes, composite polymer electrolytes and blend based polymer electrolytes have emerged. The change in the structure of polymers can be studied by doping the transition metal ions. PVC is a commercially available, inexpensive polymer and

\* e-mail: [chramu8@gmail.com](mailto:chramu8@gmail.com)

is compatible to a large number of transition metals. We have directed our attention to PVC as a host polymer of polymer electrolytes as it is possible to achieve impressive enhancement of material properties such as increased thermal stability and improved mechanical properties compared to the pure polymers, especially when these properties depends on dopant concentration. Manganese is well known magneto-active multivalent element; thus its halides can be used as fillers to modify the electric conduction and optical absorption of polymer matrix. However, no work has been reported so far on  $Mn^{2+}$  doped PVC films. Hence, the authors have taken up the investigation. The major aim of this study is to investigate a wide range of the physical properties of PVC films by doping with different concentrations of  $Mn^{2+}$ .

## 2. Experimental Part

Poly(vinyl chloride) (PVC) has a mean relative molecular mass of about 534,000 g/mol. PVC polymer films doped with  $MnSO_4$  in various concentrations were prepared at room temperature by solution cast method. The desired concentration of  $MnSO_4$  solutions (1, 2, 3, 4 and 5 mol%) were prepared by using distilled water. 1 gram of PVC polymer is dissolved in 10 ml of tetrahydrofuran (THF) separately. Different amounts of  $MnSO_4$  solution (1, 2, 3, 4 and 5 mol%) were added into the polymer solution. The mixture solution was magnetically stirred for 10-12 hours to get homogeneous mixture and then cast onto poly propylene dishes. The film was slowly evaporated at room temperature to obtain free standing polymer film at the bottom of the dishes.

In order to investigate the nature of the polymer films, differential scanning calorimetry (DSC) measurement was carried out by a SIEKO calorimeter (DSC-220) a continuous heating rate of 10 °C/min under nitrogen atmosphere from 50 to 400 °C. The thermogravimetric analysis (TGA) was done using the SEIKO thermal analysis (TGA-20) system in the presence of nitrogen flow from 50 to 500 °C, at the heating rate of 10 °C/min. X-ray diffraction measurements were carried out using a BRUKER D8 ADVANCE diffractometer with  $CuK\alpha$  radiation (1.5406 Å). The films were scanned at 2 $\theta$  angles between 10° and 80° with a step size of 0.02°. FTIR spectra of these films were recorded using the NICOLET 5700 FTIR spectrophotometer. The spectra were taken over a wavenumber range of 400-4000  $cm^{-1}$ . EPR spectra were recorded at room temperature on a JEOL FEIX ESR Spectrometer operating in X-band frequency of 9.86 GHz with a field modulation of 100 KHz. The magnetic field was scanned from 0 to 5000 G. UV-Vis absorption spectra of prepared samples were recorded in the range 200-900 nm at room temperature using JASCO UV-VIS-NIR spectrophotometer (model- V.700). From the optical absorption data, the optical constants such as band edge, optical band gap (both direct and indirect) were calculated.

The morphology of the polymer films was characterized by the JEOL JSM 840A electron microscope (SEM)

## 3. Results and Discussions

### 3.1. Differential scanning calorimetry

DSC is used to measure the enthalpy changes that occur in a sample as a function of temperature. Using this technique, the glass transition temperature ( $T_g$ ) as well as melting temperature ( $T_m$ ) and degree of crystallinity of the material can be identified. Figure 1 shows the DSC thermograms of pure and  $Mn^{2+}$  doped PVC films, showing a glass transition temperature at 80 °C. Louise – Anne. F et al.<sup>19</sup> reported glass transition temperature of pure PVC around 80 °C. Earlier Janaki Rami Reddy et al<sup>20</sup>. reported glass transition temperature of 81 °C for pure PVC films. The endothermic peak observed in the samples (Figure 1 (a), (b), (c) & (d)) at 51 °C may be due to the presence of small traces of THF.

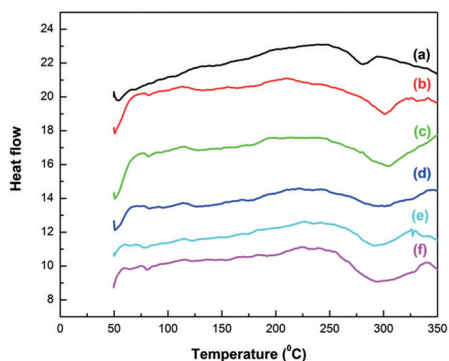


**Figure 1:** DSC curves of PVC polymer films containing  $Mn^{2+}$  (a) pure (b) 1mol% (c) 2 mol% (d) 3 mol% (e) 4 mol% (f) 5 mol%.

From Figure 1 it can be seen that all the samples exhibit only one  $T_g$  which indicates the homogeneous behaviour of polymer film<sup>21</sup>. An endothermic peak has been observed around 280 °C and 300 °C for pure, and  $Mn^{2+}$  doped PVC films respectively, which corresponds to the dehydrochlorination of PVC. A slight shift of  $T_m$  towards higher temperature on the addition of  $Mn^{2+}$  ions to the polymer reveals the disruption of crystallinity of the polymer<sup>21</sup>. On increasing doping concentration, the broadening of the melting endothermic peak is a clear indication of decrease in the degree of crystallinity and dominant presence of amorphous phase<sup>22</sup>. This clearly indicates that the micro movement of the PVC chain becomes easier by the addition of the  $Mn^{2+}$  ions, presumably owing to the decrease in crystallinity of these polymers. This establishes polar attractive forces between the ions and the chain segments thereby increasing the

segmental mobility. The melting temperature ( $T_m$ ) is taken at the apex of the melting endothermic peak as shown in Figure 1 the point where the polymer gets completely melted. The melting temperature ( $T_m$ ) of Mn<sup>2+</sup> doped (1 and 2 mol%) PVC shifted to higher temperatures. The highering of  $T_m$  upon Mn<sup>2+</sup> addition is due to the increase in spherulite sizes and their surface free energy. When Mn<sup>2+</sup> concentration further increases  $T_m$  is lowered, due to the suppression of crystallites, there by increasing the amorphous content in the polymer. As a result of more flexible amorphous environment getting trapped in or adjacent to the crystalline matrix, the suppressed crystalline portion of the Mn<sup>2+</sup> doped PVC melts probably at lower temperatures. The smaller crystallites, due to the presence of Mn<sup>2+</sup>, are less stiff to give a low  $T_m$  and consequently the amorphous phase become more flexible<sup>23</sup>.

### 3.2. Thermogravimetric Analysis

Thermogravimetric analysis (TGA) is one of the powerful tools in determining the stability of polymer and its dopants. TGA is the most widely used thermal method. It is based on the measurement of mass loss of material as a function of temperature or time in a controlled atmosphere. In thermogravimetric a continuous graph of mass change against temperature is obtained when a substance is heated at a uniform rate or kept at constant temperature. Two types of thermal decomposition processes are usually recognized in polymers, chain de-polymerization and random decomposition. Chain de-polymerization is the release of monomer units from a chain end or at a weak link and is essentially the reverse process of polymerization. It is often called de-propagation or unzipping. Random degradation occurs by chain rupture at random points along the chain, giving a disperse mixture of fragments. Both processes cause sample mass losses at certain high temperatures.

Figure 2 shows the TGA curves of pure and Mn<sup>2+</sup> doped PVC films at different concentrations (1, 2, 3, 4 and 5 mol%). Thermal stability is represented by the weight loss of the sample after heating over the temperature range 40–400 °C. Analysis of TGA curves reveals that there are three distinct steps of degradation. A first degradation was observed from 60 to 90 °C with a weight loss of 5% which may be due to THF evaporation. The weight loss curves showed degradation of samples above 260 °C in two steps. The major degradation in the temperature range 260–310 °C is attributed to dehydrochlorination<sup>24</sup>. Molecular reaction and radical propagation reactions become more probable and contribute to the cleavage of C - Cl bond. At temperature higher than 310 °C the chain radical mechanism becomes relevant and the melting of C - C or C - H bonds takes place. The degradation temperature increases with increasing dopant concentration. Probably, the presence of manganese strengthens the van der Waals interactions between the PVC chains, which leads to increased decomposition temperature. The source of the incomplete decomposition at high dopant content is not clear, but is believed to be associated with the Cl<sup>-</sup> anion containing backbone<sup>25,26</sup>.

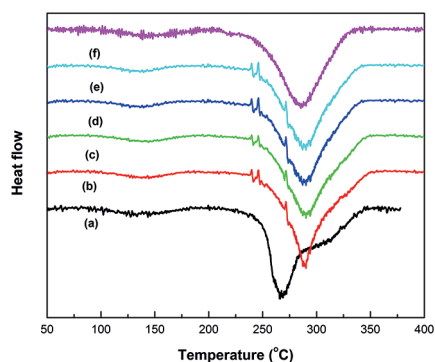


**Figure 2:** dTG curves of PVC polymer films containing Mn<sup>2+</sup> (a) pure (b) 1mol% (c) 2 mol% (d) 3 mol% (e) 4 mol% (f) 5 mol%.

### 3.3. X-ray diffraction analysis

XRD patterns of pure PVC and Mn<sup>2+</sup> doped films are shown in Figure 3. PVC exhibits a maximum intensity peak at 12°, next peak at 25° and a relatively less intense peak at 41° respectively. Peak at 12° for pure PVC has slightly shifted in doped polymer films. This indicates that the addition of Mn<sup>2+</sup> causes a decrease in the degree of crystallinity and a simultaneous increase in the amorphicity of the doped films. The comparative study reveals that the intensity of all crystalline peaks of PVC decreases gradually upon the addition of Mn<sup>2+</sup> ions to the polymer. But in 5 mol% Mn<sup>2+</sup> ion doped film, the intensity has decreased compared to values from 1 to 4 mol%. This could be due to the disruption of the semi crystalline structure of the film by Mn<sup>2+</sup> ions. When MnSO<sub>4</sub> dissolves in the polymer, the interaction between PVC and Mn<sup>2+</sup> leads to a decrease of the intermolecular interaction among the polymer chains which reduces the crystalline phase and hence increases the amorphous region. The relative intensities of peaks of PVC at around 15° and 25° with 5 mol% Mn<sup>2+</sup> are different from those of pure PVC, which indicates that the dopant inhibits the orientation of PVC crystallites preferentially in certain directions<sup>27</sup>. Hence 5 mol% is considered to be optimum value with the concentration. This amorphous nature results in greater ionic diffusivity with a high ionic conductivity which can be obtained in amorphous polymer that have flexible backbone<sup>28</sup>. The low intensity broad peaks observed around 25° and 41° which are attributed to the amorphous nature of PVC<sup>29-31</sup>. The sample with 1 mol% Mn<sup>2+</sup>, the intensity of the peak observed at 12° has been increased, which may be due to increased crystallinity. These observation confirm that the present polymer possesses both crystalline and amorphous regions.

### 3.4. Fourier Transform Infrared Spectroscopy

FTIR is a technique used to obtain information about the chemical bonding in a material. It is used to identify the elemental constituents of a material. FTIR spectra of pure

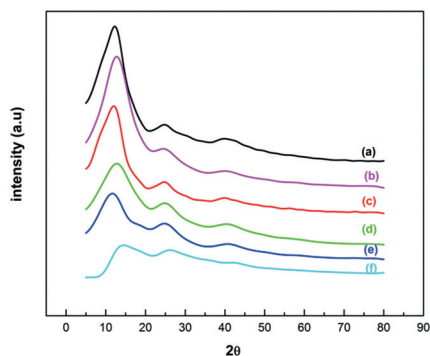


**Figure 3:** XRD patterns of PVC polymer films containing  $\text{Mn}^{2+}$  (a) pure (b) 1mol% (c) 2mol% (d) 3 mol% (e) 4 mol% (f) 5 mol%.

and  $\text{Mn}^{2+}$  (1, 2, 3, 4 and 5 mol%) doped PVC polymer films are shown in Figure 4. The FTIR spectrum of pure PVC exhibits several bands characteristic of stretching and bending vibrations of C – Cl, C – H, C = C and O – H groups. As observed from Figure 4 the characteristic bands of pure PVC can be classified into three regions. The first is the C – Cl stretching region in the range of 600 – 700  $\text{cm}^{-1}$ . The second region is C – C stretching in the range from 900 – 1200  $\text{cm}^{-1}$ . The third region is 1250 – 2970  $\text{cm}^{-1}$  in PVC<sup>32</sup> (numerous CH modes). In the pure PVC spectrum, the bands at 1333, 1254, and 950  $\text{cm}^{-1}$  are assigned to  $\text{CH}_2$  deformation, CH rocking and CH wagging of PVC respectively<sup>33</sup>.

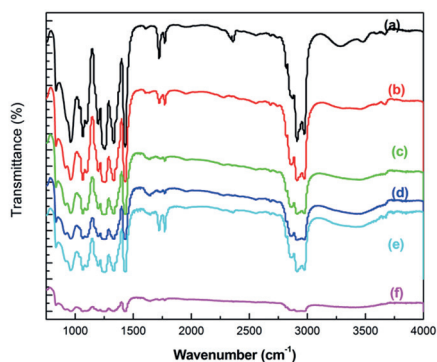


**Figure 4:** FTIR patterns of pure and  $\text{Mn}^{2+}$  doped PVC polymer films (a) pure (b) 1mol% (c) 2 mol% (d) 3 mol% (e) 4 mol% (f) 5 mol%.

From the Figure 4 the following changes in the spectral feature have been observed on comparing  $\text{Mn}^{2+}$  doped PVC with that of the pure PVC. The strong broad absorption band appearing in the 2769 – 3088  $\text{cm}^{-1}$  region in pure PVC corresponds to symmetric and asymmetric C – H stretching modes of the  $\text{CH}_2$  groups<sup>34</sup>. With increasing dopant concentration the width increases and intensity of these bands in PVC is found to decrease. The broad absorption peak around

3284  $\text{cm}^{-1}$  and a sharp peak at 1713  $\text{cm}^{-1}$  observed in pure PVC, which were attributed to the OH molecule which may be due to the presence of THF, almost disappeared in the doped films. This indicates the complete exchange of basal cations with the removal of water molecules<sup>35</sup>. The vibrational peak observed at 2352  $\text{cm}^{-1}$  of pure PVC is found to absent in  $\text{Mn}^{2+}$  doped films. The disappearance of bands observed in pure films with  $\text{Mn}^{2+}$  doping suggests the co-ordination or complexation of  $\text{Mn}^{2+}$  ions to the chlorine of PVC<sup>36</sup>.

The FTIR spectrum of PVC:  $\text{Mn}^{2+}$  (1, 2, 3, 4 and 5 mol%) films exhibit bands, whose vibrational frequencies and band assignments are found to be similar to several bands observed for undoped PVC but O – H stretching frequency observed at 3284  $\text{cm}^{-1}$  for pure PVC shows remarkable shift towards high frequency region on doping of  $\text{Mn}^{2+}$  ions. These changes indicate the possibility of  $\text{Mn}^{2+}$  ion to be attached to O – H groups in the side chain of PVC molecule<sup>37</sup>.

### 3.5. Optical Analysis

Measurement of the absorption spectrum is the most direct and simplest method for investigating the band structure of materials. In the absorption process an electron is excited from a lower to higher energy state by absorbing a photon of known energy in the transmitting radiation. The changes in the transmitted radiation can decide the types of possible electron transitions. Fundamental absorption refers to band-to-band or exciting transition. Furthermore the fundamental absorption manifests itself by a rapid rise in absorption, known as absorption edge, which can be used to determine the optical band gap. Insulators/semiconductors are generally classified into two types: (a) direct band gap and (b) indirect band gap. In direct band gap semiconductors, the top of the valence band and the bottom of the conduction band both lie at same zero crystal momentum (wave vector). If the bottom of the conduction band does not correspond to zero crystal momentum, then it is called indirect band gap semiconductor. In indirect band gap materials transition from valence to conduction band should always be associated with a phonon of the right magnitude of crystal momentum. Davis and Shalliday<sup>38</sup> reported that near the fundamental band edge both direct and indirect transitions occur and can be observed by plotting  $\alpha^{1/2}$  and  $\alpha^2$  as a function of energy (hv).

Optical absorption spectra of pure and various concentrations of  $\text{Mn}^{2+}$  ions doped PVC polymer films are shown in Figure 5. The spectrum of pure PVC film shows a peak at 286 nm which is assigned to the carbonyl group of PVC. In doped film the intensity of this peak is increased as the absorption coefficient increases as doping level increases. This may be due to the string interaction between PVC and  $\text{Mn}^{2+}$  ions<sup>39</sup>.

The absorption coefficient  $\alpha$  can be determined from the spectra using the formula.

$$\alpha = \left( \frac{A}{d} \right) * 2.303 \quad (1)$$

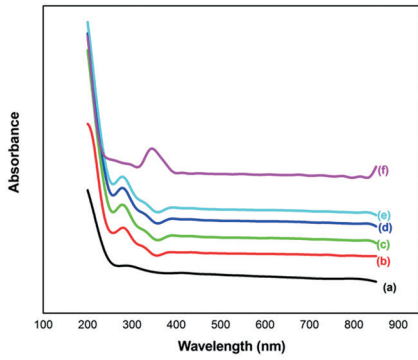


**Figure 5:** UV-Vis absorption spectra of pure and Mn<sup>2+</sup> doped PVC polymer films (a) Pure (b) 1mol % (c) 2 mol % (d) 3 mol % (e) 4 mol% (f) 5 mol%.

Where A is the absorption and d is the thickness of the sample. The position of absorption edge was estimated by extrapolating the linear portion of the  $\alpha$  vs.  $h\nu$  (Figure 6) to zero absorption value. For pure PVC film the absorption edge lies at 4.52 eV and for doped film the values are found to decrease from 4.46 to 4.20 eV. When direct band gap exists, the absorption coefficient has the following dependence on the energy of the incident photon<sup>40</sup>.

$$\alpha h\nu = c(h\nu - E_g)^{\frac{1}{2}} \quad (2)$$

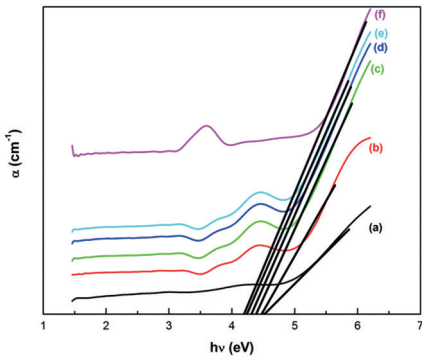


**Figure 6:**  $\alpha$  vs  $h\nu$  plots of pure and Mn<sup>2+</sup> doped PVC polymer films (a) Pure (b) 1mol % (c) 2 mol % (d) 3 mol % (e) 4 mol% (f) 5 mol%.

Where  $E_g$  is the band gap, C is constant, is the frequency of light and  $h$  is the Planck's constant. The intercept on the energy axis on extrapolating the linear portion of the curves to zero absorption value may be interpreted as the value of direct band gap (Figure 7). For pure PVC film the direct band gap lies at 5.26 eV while for Mn<sup>2+</sup> doped films the values are found to decrease from 5.23 to 5.06 eV (Table 1). For indirect transitions, which require photon assistance, the

absorption coefficient has subsequent dependence on the photon energy<sup>40</sup>.

$$\alpha h\nu = A(h\nu - E_{h_g} + E_p)^2 + B(h\nu - E_g - E_p)^2 \quad (3)$$

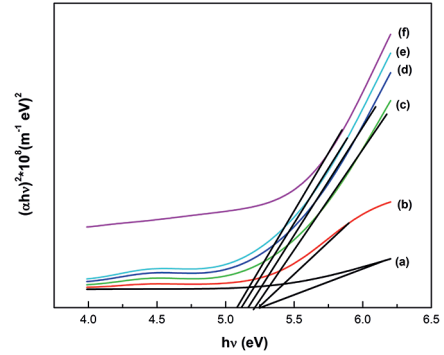


**Figure 7:**  $(\alpha h\nu)^2$  vs  $h\nu$  plots of pure and Mn<sup>2+</sup> doped PVC polymer films (a) Pure (b) 1mol % (c) 2 mol % (d) 3 mol % (e) 4 mol% (f) 5 mol%.

**Table 1:** Absorption edge, optical band gap values of pure and Mn<sup>2+</sup> ions doped PVC polymer films

PVC: Mn <sup>2+</sup> Concentration (mol %)	Absorption edge (eV)	Optical band gap energy (eV)	
		Direct	Indirect
Pure	4.52	4.89	4.25
1	4.46	4.87	4.15
2	4.39	4.83	3.87
3	4.31	4.77	3.74
4	4.25	4.73	3.66
5	4.20	4.58	3.60

Where  $E_p$  is the energy of the photon associated with the transition and A and B are constants depending on the band structure. The indirect band gaps were obtained from the plots of  $(\alpha h\nu)^{1/2}$  vs.  $h\nu$  as shown in Figure 8. For pure PVC polymer film the indirect band gap lies at 4.25 eV while for Mn<sup>2+</sup> doped films, the values are found to decrease from 4.15 to 3.60 eV. These values are presented in Table 1 together with absorption edge values, the direct band gap and indirect band gap energies obtained from absorption spectra.

The optical band gap energies of the pure PVC and Mn<sup>2+</sup> doped samples observed in the present work indicate the semiconducting nature of these samples. From Table 1, it is evident that the optical band gap energy goes on decreasing with increasing Mn<sup>2+</sup> content. This indicates that with increase in concentration of Mn<sup>2+</sup> ions, PVC film becomes more semiconducting in nature<sup>37</sup>.

### 3.6. Scanning Electron Microscopy

Scanning electron microscopy (SEM) is often used to study the compatibility between various components of

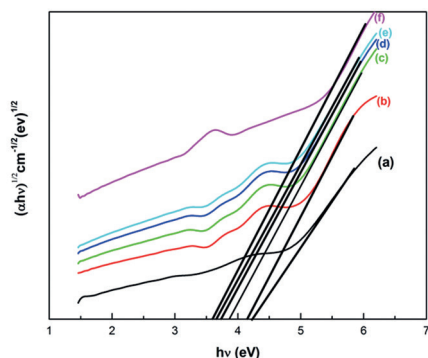


**Figure 8:**  $(\alpha hv)^{1/2}$  vs  $h\nu$  plots of pure and  $Mn^{2+}$  doped PVC polymer films (a) Pure (b) 1 mol % (c) 2 mol % (d) 3 mol % (e) 4 mol% (f) 5 mol%.

polymer films through the detection of phase separations and interfaces<sup>41,42</sup>. The compatibility between the polymer matrix and dopants has great influence on the properties (mechanical, thermal, ionic conductivity) of the polymer films. Also topography study of the samples gives important information regarding the growth mechanism, shape and size of the particles.

The morphology of the pure and  $Mn^{2+}$  (1, 2, 3, 4 and 5 mol%) doped polymer films, studied by SEM technique, is a uniform type but with different degrees of roughness. The pure and doped films were observed at the same magnification. Figure 9 shows the surface morphology of doped polymer film with different concentrations of  $Mn^{2+}$  ions. When  $Mn^{2+}$  ions are added to the polymer the surface morphology of pure PVC changes from smoother to rumples. This indicates the semi-crystalline nature of polymer by the addition of  $Mn^{2+}$  ions. As the dopant concentration increases, the rumples are gradually increasing and the surface morphology is further improved.

In Figure 9 (a & b), micrograph illustrates the existence of randomly distributed microcrystallites of grain like shape as a common feature of the studied film. In Figure 9 (c & d) several spherical pores, which have formed on the surface, are due to the rapid evaporation of the solvent (THF). The difference in the pore size is related to the difference in the driving force for phase separation<sup>13</sup>. It can be seen from Figure 9 (e) that 4 mol% has better spherical pore surface distribution than Figure 9 (c & d). It can be inferred that the polymer matrix is in homogenous condition. As a result, the charge carriers can be transported quickly and easily without the presence of blocking phase and hence the highest ionic conductivity is observed. The highest ionic conductivity is also ascribed to the highest porosity.

In Figure 9 (f), i.e., with 5 mol%  $Mn^{2+}$ , hardness of the composites increased with the percentage of the  $Mn^{2+}$ .

Thus increase in  $Mn^{2+}$  concentration promotes a continuous network formation. It can be seen that with the doping of  $Mn^{2+}$  the morphology of the sample changes to hexagonal shape. The hexagonal shape acts as a short-term stabilizer and the  $Mn^{2+}$  doped PVC acted not only as a long-term stabilizer because of hydroxyl, but also a short-term one due to  $Mn^{2+}$ . However, with the content of  $Mn^{2+}$ , the performance of long-term stabilizer was weakens, which can enhance the stability of PVC greatly<sup>36</sup>.

### 3.7. Electron paramagnetic resonance studies

The EPR spectroscopy has been used as a tool to elucidate the structural evolution of materials. We used divalent Mn probe;  $Mn^{2+}$  is a sensitive indicator of structural changes owing to its unshielded  $d^5$  ions. Host-activator compositions are of considerable interest for elucidating the structure and bonding in vitreous (isotropic) and crystalline (anisotropic) system.

The EPR spectra of  $Mn^{2+}$  ions doped PVC polymer films have been studied systematically as a function of  $Mn^{2+}$  content varying from 1 to 5 mol% and are shown in Figure 10. The observed signals are characterized by the following features. For undoped PVC, the EPR spectrum can be accounted for the presence of a broad single line spectrum at  $g = 2.48$  (Figure 10 inset), this broad single line arose from coupling of the unpaired electron spin and a large number of protons<sup>39</sup>.

For  $Mn^{2+}$  doped PVC, the EPR spectra exhibit a strong and sharp signal located at  $g$  value of 1.90, which has been overlapped with the  $g = 2.48$  signal, indicating the presence of aggregated  $Mn^{2+}$ . The intensity of the signal is larger for 5 mol%, indicating a very large concentration of  $Mn^{2+}$  ions in the polymeric matrix<sup>43</sup>.

At the concentration of  $Mn^{2+}$  ions varying from 1 to 5 mol%, the unresolved hyperfine lines related  $Mn^{2+}$  ions were vague and nearly disappeared suggesting a decrease the content of the isolated  $Mn^{2+}$  ions from one part and increase the content of aggregated  $Mn^{2+}$  ions from the second part indicating the existence of interacting paramagnetic centres  $Mn^{2+}$  ions that interact with other  $Mn^{2+}$  ions<sup>44</sup>.

The number of  $Mn^{2+}$  ions participating in resonance can be calculated by comparing the area under the absorption curve with that of a standard one ( $MnSO_4 \cdot 5H_2O$  in this study) of known concentration. The number of spins ( $N$ ) participating in the resonance was roughly estimated by the equation.

$$N = I * (\Delta H_{pp})^2$$

Figure 11 shows the number of spins participating in resonance in PVC as a function of  $MnSO_4$  content at room temperature. It is observed that the number of spins participating in resonance increase with increase in  $MnSO_4$  content. It is observed that in the present study, the intensity of EPR signal steadily increases with  $MnSO_4$  content.

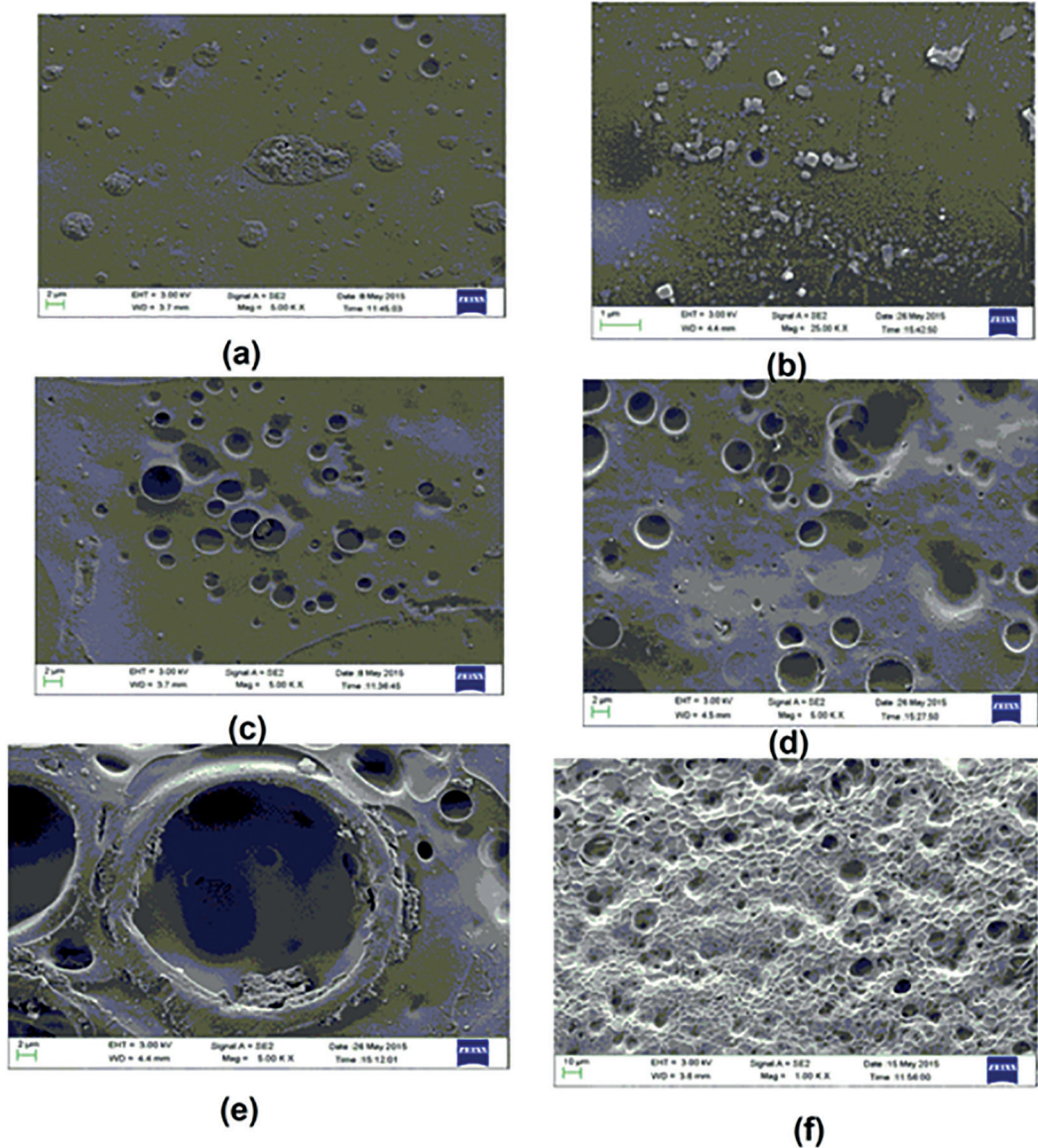


**Figure 9:** SEM photographs of pure and Mn<sup>2+</sup> doped PVC polymer films (a) pure (b) 1 mol% (c) 2 mol% (d) 3 mol% (e) 4 mol% (f) 5 mol%.

The ESR data can be used to calculate the paramagnetic susceptibility<sup>43</sup> of the sample using the formula.

$$X = N^2 g \beta^2 J(J + 1) / 3K_B T$$

Where N is the number of spins per m<sup>3</sup>, J is the total angular momentum quantum number,  $\beta$  is the Bohr magnetron,  $k_B$  is the Boltzmann constant, T is the absolute temperature and g is the land'e g factor. Using the above equation, the paramagnetic susceptibility was calculated as a function of dopant concentration and is shown in Figure 11. As observed in the plot, paramagnetic susceptibility increases with MnSO<sub>4</sub> concentration.

#### 4. Conclusions

Pure and Mn<sup>2+</sup> doped PVC polymer films were prepared using the solution cast technique. Pure PVC thermogram shows two-step decomposition and the thermal degradation of polymer samples involves an additional step when Mn<sup>2+</sup> ions are added. The melting temperature  $T_m$  of Mn<sup>2+</sup> doped PVC shifts towards higher and lower temperatures. The highering of  $T_m$  is due to the increase in spherulite sizes and their surface energy, the lowering is due to the suppression of crystallites, there by increasing the amorphous content in the polymer. TGA and DSC analysis reveals that the sample is thermally stable up to 350 °C. Optical absorption edge and optical energy gaps (both direct and indirect) show a

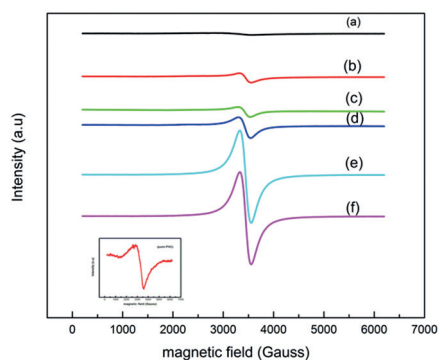


**Figure 10:** EPR spectra of pure and  $Mn^{2+}$  doped PVC polymer films (a) pure (b) 1 mol% (c) 2 mol% (d) 3 mol% (e) 4 mol% (f) 5 mol%.

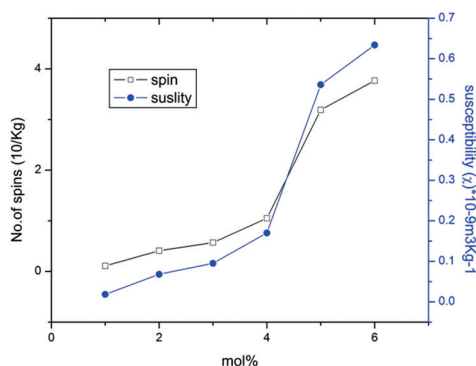


**Figure 11:** Variation of number of spins & susceptibility participating in PVC films containing  $Mn^{2+}$  ions.

decreasing trend with increasing dopant concentration. It was observed that these values shifted to lower energies on doping. This indicates that the doped PVC films become, semiconducting in nature. In SEM studies, with the doping of  $Mn^{2+}$ , the morphology of the PVC sample changes to hexagonal shape. The XRD observations confirm that the present polymer possesses multiphase, having both crystalline and amorphous regions. The observed strong and weak bands in the FTIR spectrum indicates the presence of stretching and bending vibrational modes. O-H stretching frequency shifts towards high frequency on adding  $Mn^{2+}$  ions, which indicates the possibility of  $Mn^{2+}$  ion to be attached to O-H groups in the side chain of PVC molecule.

## 5. Acknowledgments

The authors thank Dr. Tushar Jana, Associate Professor, Dept. of Chemistry, for his constant encouragement and active co-operation in carrying out the work. We also thank to

Network Resource Centre in Central University of Hyderabad for providing the facilities to carry out experimental work.

## 6. References

- Gray FM. *Solid Polymer Electrolytes: Fundamentals and Technological Applications*. New York: Wiley-VCH Publishers; 1991. 245 p.
- Ahmad S, Ahmad S, Agnihotry SA. Nanocomposite electrolytes with fumed silica in poly(methyl methacrylate): thermal, rheological and conductivity studies. *Journal of Power Sources*. 2005;140(1):151-156.
- Ramesh S, Yuen TF, Shen CJ. Conductivity and FTIR studies on PEO-LiX [ $X: CF_3SO_3^-, SO_4^{2-}$ ] polymer electrolytes. *Spectrochimica Acta Part A: Molecular and Biomolecular Spectroscopy*. 2008;69(2):670-675.
- Mediha KOK, Demirelli K, Aydogdu Y. Thermophysical Properties of Blend of Poly (Vinyl Chloride) with Poly (Isobornyl Acrylate). *International Journal of Science & Technology*. 2008;3(1):37-42.
- Warren H. Global vinyls outlook: Building on change. In *Proceedings of 30<sup>th</sup> Annual World Petrochemical Conference*; 2015 Mar 24-27; Houston, Texas, USA. p. 479-503.
- Chen G. Preparation of a poly(vinyl chloride)/layered double hydroxide nano composite with a reduced heavy-metal thermal stabilizer. *Journal of Applied Polymer Science*. 2007;106(2):817-820.
- Sabaa MW, Mohamed NA, Khalil KD, Yassin AA. Organic thermal stabilizers for rigid poly(vinyl chloride) II. Benzal thiobarbituric acid and some of its derivatives. *Polymer Degradation and Stability*. 2000;70(2):121-133.
- Heat stabilizers. *Plastics, Additives and Compounding*. 1999;1(4):24-29.
- Yang ZH, Shu WY, Long HZ, Li XH. Influence of rare earth heating stabilizer on heating stabilizing property of PVC. *Chinese Rare Earths*. 1999;20(2):60-62.
- Chithra MK, Kesavan K, Mumoorthi M, Rajendran S. Study of electrochemical behaviour on synthesized nano-composite polymer electrolyte. *Journal of NanoScience and NanoTechnology*. 2014;2(1):12-14.
- Alamgir M, Abraham KM. Li Ion Conductive Electrolytes Based on Poly(vinyl chloride). *Journal of Electrochemical Society*. 1993;140(6):L96-L97.
- Sukeshini AM, Nishimoto A, Watanabe M. Transport and electrochemical characterization of plasticized poly(vinyl chloride) solid electrolytes. *Solid State Ionics*. 1996;86-88(Part 1):385-393.
- Rhoo HJ, Kim HT, Park JK, Hwang TS. Ionic conduction in plasticized PVC/PMMA blend polymer electrolytes. *Electrochimica Acta*. 1997;42(10):1571-1579.
- Stephan AM, Thirunakaran R, Renganathan NG, Sundaram V, Pitchumani S, Muniyandi N, et al. A study on polymer blend electrolytes based on PVC/PMMA with lithium. *Journal of Power Sources*. 1999;81-82:752-758.
- Ramesh S, Arof AK. Electrical conductivity studies of poly(vinyl chloride)-based electrolytes with double salt system. *Solid State Ionics*. 2000;136-137:1197-1200.



16. Manuel Stephan A, Prem Kumar T, Renganathan NG, Pitchumani S, Thirunkara R, Muniyandi N. Ionic conductivity and FT-IR studies on plasticized PVC/PMMA blend polymer electrolytes. *Journal of Power Sources*.2000;89(1):80-87.
17. Ramesh S, Yahaya AH, Arof AK. Dielectric behaviour of PVC-based polymer electrolytes. *Solid State Ionics*.2002;152-153:291-294.
18. Subba Reddy CV, Han X, Zhu QY, Mai LQ, Chen W. Conductivity and discharge characteristics of (PVC+NaClO<sub>4</sub>) polymer electrolyte systems. *European Polymer Journal*.2006;42(11):3114 -3120.
19. Fillot LA, Hajji P, Gauthier C, Masenelli-Varlot K. U-PVC gelation level assessment, part 1: Comparison of different techniques. *Journal of Vinyl & Additive Technology*. 2006;12(3):98-107.
20. Janaki Rami Reddy T, Achari VBS, Shrama AK, Narasimha Rao VVR. Effect of plasticizer on electrical conductivity and cell parameters of (PVC+KBrO<sub>3</sub>) polymer electrolyte system. *Ionics*.2007;13(1):55-59.
21. Pavani Y, Ravi M, Bhavani S, Sharma AK, Narasimha Rao VVR. Characterization of Poly(vinyl alcohol)/potassium chloride polymer electrolytes for electrochemical cell applications. *Polymer Engineering and Science*.2012;52(8):1685-1692.
22. Reddeppa N, Sharma AK, Narasimha Rao VVR, Chen W. Preparation and characterization of pure and KBr doped polymer blend (PVC/PEO) electrolyte thin films. *Microelectronic Engineering*.2013;112:57-62.
23. Ramesh Prabhu M, Sudalaimuthu K, Rajendran S. Investigations on PVC/PMMA blends with various lithium salts. *Indian Journal of Research*. 2013;2(3):307-309.
24. Marongiu A, Faravelli T, Bozzano G, Dente M, Ranzi E. Thermal degradation of poly(vinyl chloride). *Journal of Analytical and Applied Pyrolysis*. 2003;70(2):519-553.
25. Baskaran R, Selvasekarapandian S, Kuwata N, Kawamura J, Hattori T. Structure, thermal and transport properties of PVAc-LiClO<sub>4</sub> solid polymer electrolytes. *Journal of Physics and Chemistry of Solids*.2007;68(3)407-412.
26. Barbosa PC, Rodrigues LC, Silva MM, Smith MJ. Characterization of pTMC<sub>n</sub>LiPF<sub>6</sub> solid polymer electrolytes. *Solid State Ionics*.2011;193(1):39-42.
27. Dey A, Karan S, De SK. Effect of nanofillers on thermal and transport properties of potassium iodide-polyethylene oxide solid polymer electrolyte. *Solid State Communications*.2009;149(31-32):1282-1287.
28. Mohamad AA, Mohamad NS, Yahya MZA, Othman R, Ramesh S, Alias Y, et al. Ionic conductivity studies of poly(vinyl alcohol) alkaline solid polymer electrolyte and its use in nickel-zinc cells. *Solid State Ionics*.2003;156(1-2):171-177.
29. Morita M, Araki F, Yoshimoto N, Ishikawa M, Tsutsumi H. Ionic conductance of polymeric electrolytes containing lithium salts mixed with rare earth salts. *Solid State Ionics*. 2000;136-137:1167-1173.
30. Li XG, Kressel, Spinger J, Nissen J, Yang YL. Morphology and gaspermselectivity of blend membranes of poly vinyl pyridine with ethyl cellulose. *Polymer*.2001;42(16):6859-6869.
31. Liu C, Xiao C, Liang H. Properties and structure of PVP-lignin "blend films". *Journal of Applied Polymer Science*.2005;95(6):1405-1411.
32. Rajendran S, Ramesh Prabhu M, Usha Rani M. Characterization of PVC/PEMA Based Polymer Blend Electrolytes. *International Journal of Electrochemical Science*.2008;3(3):282-290.
33. Reddeppa N, Sharma AK, Narasimha Rao VVR, Chen W. AC conduction mechanism and battery discharge characteristics of (PVC/PEO) polyblend films complexed with potassium chloride. *Measurement*.2014;47:33-41.
34. Mohan VM, Raja V, Sharma AK, Narasimha Rao VVR. Ion transport and battery discharge characteristics of polymer electrolyte based on PEO complexed with NaFeF<sub>4</sub> salt. *Ionics*.2006;12(3):219-226.
35. Abulyazied DE, Mokhtar SM, Motawie AM. Nanoindentation behavior and physical properties of poly(vinyl chloride)/styrene co-maleic anhydride blend reinforced by nano-bentonite. *IOSR Journal of Applied Chemistry*.2015;7(12):32-44.
36. Rahman MYA, Ahmad A, Lee TK, Farina Y, Dahlan HD. Effect of ethylene carbonate (EC) plasticizer on poly(vinyl chloride)-liquid 50% epoxidised natural rubber (LENR50) based polymer electrolyte. *Material Sciences and Applications*.2011;2(7):817-825.
37. Hemantha Kumar GN, Lakshmana Rao J, Gopal NO, Narasimhulu KV, Chakradhar RPS, Varada Rajulu A. Spectroscopic investigations of Mn<sup>2+</sup> ions doped poly(vinyl alcohol) films. *Polymer*.2004;45(16):5407-5415.
38. Davis PW, Shilliday TS. Some Optical Properties of Cadmium Telluride. *Physical Review*.1960;118(4):1020-1022.
39. Abdelaziz M. Electron spin resonance and optical studies of poly(methylmethacrylate) doped with CuCl<sub>2</sub>. *Journal of Applied Polymer Science*.2008;108(2):1013-1020.
40. Thutupalli GKM, Tomlin SG. The optical properties of thin films of cadmium and zinc selenides and tellurides. *Journal of Physics D: Applied Physics*.1976;9(11):1639-1646.
41. Zhang S, Lee JY, Hong L. Visualization of particle distribution in composite polymer electrolyte systems. *Journal of Power Sources*.2004;126(1-2):125-133.
42. Chu PP, Reddy MJ. Sm<sub>2</sub>O<sub>3</sub> Composite PEO solid polymer electrolyte. *Journal of Power Sources*. 2003;115(2):288-294.
43. El-Khodary A. Evolution of the optical, magnetic and morphological properties of PVA films filled with CuSO<sub>4</sub>. *Physica B: Condensed Matter*.2010;405(16):3401-3408.
44. Linga Raju Ch, Rao JL, Gopal NO, Reddy BCV. Electron paramagnetic resonance and optical absorption studies of Cu<sup>2+</sup> ion doped poly(vinyl alcohol) films. *Materials Chemistry and Physics*. 2007;101(2-3):423-427.